SRF

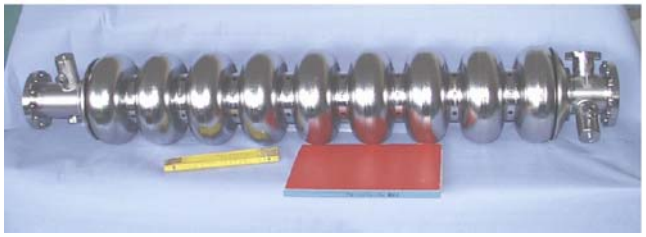

Deliverable 11.2.13:

"Evaluation of beam emittance monitor operation: Optical Diffraction Radiation Based Non-Intercepting Beam Size Monitor"

M. Castellano[1], E. Chiadroni[1], A. Cianchi[2] , K. Honkavaara[3], G. Kube[3]

1) INFN-Laboratori Nazionali di Frascati – INFN, via E. Fermi, 40, 00044 Frascati, Italy
2) INFN- Sezione di Tor Vergata e Universita` di Roma ''Tor Vergata'', via della Ricerca Scientifica, 1, 00133 Roma, Italy
3) Deutsches Elektronen-Synchrotron, Notkestraße 85, 22607 Hamburg, Germany

Abstract

The characterization of the transverse phase space for high charge density and high energy electron beams is demanding for the successful development of the next generation light sources and linear colliders.

The interest in a non-invasive and non-intercepting beam diagnostics is increasingly high due to the stringent features of such beams.

Optical Diffraction Radiation (ODR) is considered as one of the most promising candidates to measure the transverse beam size and angular divergence, i.e. the transverse emittance. This is our goal.

An experiment, based on the detection of the ODR angular distribution, has been set up at DESY FLASH Facility to measure the electron beam transverse parameters, in order to retrieve the normalized transverse emittance. Here difficulties are discussed which we encountered and overcame, and results obtained during the whole measurement period will be presented.

Acknowledgements

We acknowledge the support of the European Community-Research Infrastructure Activity under the FP6 "Structuring the European Research Area" programme (CARE, contract number RII3-CT-2003-506395)

1. Introduction

The development of high energy Linear Colliders (LC) [1] and short wavelength Free-Electron Lasers (FEL) [2–4] requires high quality electron beams, which means small transverse emittance (<1 mm mrad) and high peak current (≈ kA). Due to the large power density of this kind of beams, a non-intercepting diagnostics needs to be developed and applied. In 1996 one of the authors suggested a new method for the non-intercepting measurement of beam size, both transverse [5] and longitudinal [6]. The idea is based on the observation of diffraction radiation (DR) emitted by a charged particle beam going through a slit in a metallic foil due to the interaction of the charge electromagnetic (EM) field with the screen surface (Fig. 1). Since the beam goes through the slit, DR is a non-intercepting diagnostics and, therefore, excellent to be used parasitically without disturbing the electron beam. The great interest in this type of radiation [7], [8] comes also from both the possibility of generation of intense radiation beams in millimeter and sub-millimeter wavelength region and beam diagnostics based on both incoherent and coherent diffraction radiation [9], depending on the longitudinal beam size with respect to the emitted wavelength. The aim of our experiment is measuring the transverse beam size and divergence, in order to calculate the transverse emittance, by studying the angular distribution of optical diffraction radiation (ODR). The DR angular distribution is produced by the interference of radiation from both edges of the slit. The visibility of the interference fringes is correlated to the beam size (see Fig. 2, left). The effect is also affected, in a slightly different way, by the angular divergence of the beam (Fig. 2, right): the ODR angular distribution becomes wider and the intensity of the minimum higher, when the beam divergence increases as pointed out in Section 2.
A dedicated analysis of the radiation angular distribution allows then to separate the two effects. If the beam waist is located in the plane of the DR screen, the transverse emittance can be derived with a single non-intercepting measurement.

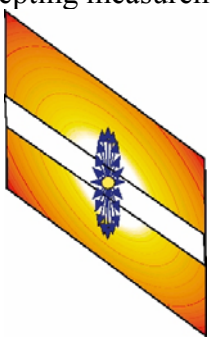

Fig. 1 – Sketch of the EM field of a charged particle and its interaction with a metallic screen with a cut.

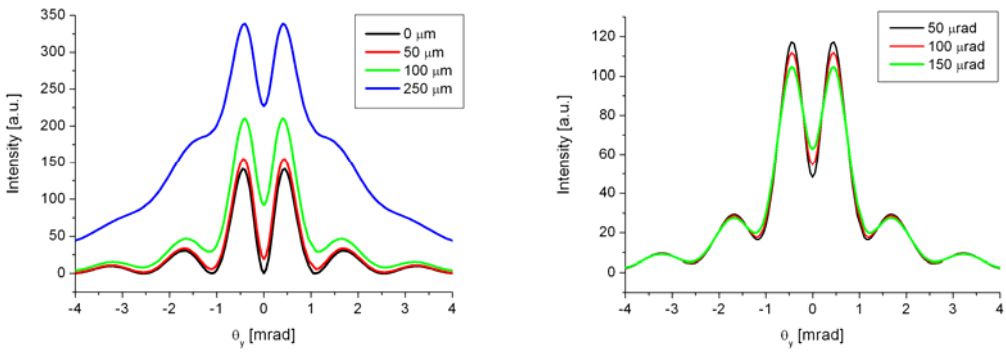

Fig. 2 – Theoretical calculation for the angular distribution of the vertical component of ODR for different transverse beam sizes (left) and angular divergences (right). The simulation has

been performed assuming an electron beam energy of 680 MeV, with interference filter (800 nm) and 0.5 mm slit width.

2. – Diffraction Radiation Theory

Diffraction radiation is produced when a charged particle goes through a slit or passes close to the edge of a metallic screen, due to the interaction between the EM field of the traveling charge and the target surface [10]. The intensity of the radiation increases linearly with the charge and is proportional to $e^{-2\pi a/\gamma\lambda}$, where a is the slit aperture, γ the Lorentz factor and λ the emitted wavelength. A natural unit of measure of this phenomenon is given by the radial extension of the EM field, $\gamma\lambda/2\pi$. In case of $a >> \gamma\lambda/2\pi$, the aperture is much larger than the extent of the particle EM field, which does not interact with the target at all and, therefore, no radiation is produced. In the opposite case, if $a << \gamma\lambda/2\pi$, transition radiation is substantially emitted. In the following we treat the case of $a \approx \gamma\lambda/2\pi$ resulting in the emission of DR. Typically, the transverse beam size is of the order of mm or sub-mm. This means that in case of high energy, $\gamma \approx 10^3$, also optical wavelengths are emitted, allowing an easier detection of radiation, thanks to the wide instrumentation available in the optical range. The transverse beam parameters like position, transverse size, angular divergence can then be reconstructed from the emitted optical DR angular distribution.

The radiation emission mechanism can be described by the Weizsäcker–Williams method or virtual photon method [10]. The EM field of an ultra-relativistic ($\gamma >> 1$) particle acquires the properties of electromagnetic waves, allowing to be approximated as a superposition of plane waves (virtual photons), and can be written as

$$E^0_{x,y}(\omega, x, y, z) = \frac{e\omega}{\pi v^2 \gamma} \frac{x, y}{\sqrt{x^2 + y^2}} K_1\left(\frac{\omega\sqrt{x^2 + y^2}}{v\gamma}\right) e^{i\frac{\omega}{v}z} \quad (1)$$

with K_1 the modified Bessel function of second order. The electric field transverse components are then proportional to $\xi K_1(a\xi)$, with $\xi = \omega/(\gamma v)$. A strong field is then detected and DR emitted if $a\xi = \frac{a\omega}{\gamma v} = \frac{2\pi a}{\gamma\lambda} \leq 1$, where $\beta \approx 1$ has been considered. As consequence, radiation is confined within a disk of radius $\gamma\lambda$ and, contrary to the plane EM wave, the particle field depends on the distance from it. The diffraction radiation field can, therefore, be considered as the scattering of the virtual photon field on the metallic target. The radiated energy is determined by solving the Kirchoff integral [11] which, in the far field approximation, can be considered as the Fourier transform of the field of virtual photons on the target surface. The ODR far field angular distribution in the Fraunhofer approximation is given by

$$E_{x,y}(k_x, k_y) = -\frac{1}{(2\pi)^2} \int_S E^0_{x,y}(x, y) e^{-i(k_x x + k_y y)} dS \quad (2)$$

where k_x and k_y are the transverse components of the radiation momentum $k = \omega/c$ and $E^0_{x,y}$ the fields on the metallic surface given by Eq.1. For an electron moving through the center of a slit in a perfectly conducting, infinite screen, the expression for both polarizations, parallel and orthogonal to the slit, have the form

$$E_x(k_x,k_y)=\frac{iek_x}{4\pi^2cf}\left\{\frac{e^{-\frac{a}{2}\left(f-ik_y\right)}}{f-ik_y}+\frac{e^{-\frac{a}{2}\left(f+ik_y\right)}}{f+ik_y}\right\}$$
$$E_y(k_x,k_y)=\frac{ie}{4\pi^2c}\left\{\frac{e^{-\frac{a}{2}\left(f-ik_y\right)}}{f-ik_y}-\frac{e^{-\frac{a}{2}\left(f+ik_y\right)}}{f+ik_y}\right\} \quad (3)$$

where $f=\sqrt{k_x^2+\frac{\omega^2}{(\gamma v)^2}}$. The DR spectral angular distribution is then given by

$$\frac{d^2U}{d\omega d\Omega}=\frac{d^2U_{\parallel}}{d\omega d\Omega}+\frac{d^2U_{\perp}}{d\omega d\Omega}=\frac{1}{4\pi\varepsilon_0}\frac{\omega^2}{4\pi^2c}\left(\left|E_x\right|^2+\left|Ey\right|^2\right). \quad (4)$$

The angular distribution of the DR is mainly affected by beam parameters in the plane orthogonal to the slit aperture: when the transverse beam size is increased, the intensity of both the peaks and the minima increases, resulting in the reduction of the interference fringes visibility, as stated by a simulation plotted in Fig. 2 (left). Keeping in mind that the radiation angular distribution is centered around the direction of specular reflection of the particle trajectory, to evaluate the effect of the angular divergence for a real beam the DR angular distribution is convoluted with a 1D Gaussian distribution over the variable y, i.e.

$$f(y,\sigma'_y)=\frac{1}{\sqrt{2\pi}\sigma'_y}e^{-\frac{y^2}{2\sigma'^2_y}}. \quad (5)$$

The result of the numerical computation, shown in Fig. 2 (right), appears as a smoothing out of the maximum and minimum values as the beam angular divergence increases. In our case, the slit is a horizontal rectangular aperture, allowing to measure the beam size and the beam angular divergence in the vertical plane, σ_y and σ'_y, respectively.

3. - Experiment layout

The experiment was performed at FLASH (DESY, Hamburg) [12] on the bypass line. In order the avoid unnecessary losses in the permanent undulator magnets, the by-pass line is used to transport the electron beam to the dump , when the production of FEL radiation is not required. The location in the bypass simplified any operation on the vacuum system because of less stringent vacuum conditions.
However, the use of the bypass line implicates a natural background of the synchrotron radiation which is produced in the last dipole. As already noted in the ATF experiment [5] this background can be more intense than the ODR signal. To reduce the background we installed our monitor at about 50 m away from the last dipole (see Fig. 3).

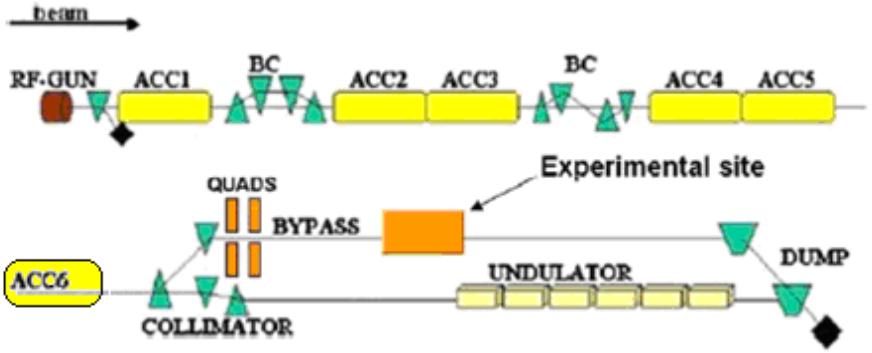

Fig. 3 – FLASH layout and experimental site

The experimental set-up consists of an aluminated silicon screen (DR screen) mounted in the vacuum pipe under an angle of 45° angle with respect to the beam direction. A dedicated optical system has been designed to guide and focus the radiation onto the camera.
The target is of fundamental importance for the success of the experiment, since damaged edges and/or an uneven surface may change the interference effects, resulting in a blurred angular distribution. Therefore, in order to avoid any kind of damages, a special care has been taken during manufacturing the target as well as during installation and measurements. The DR screen (Fig. 4) is constructed by lithographic technique starting from a silicon nitride wafer and opening two slits, 0.5 mm and 1 mm aperture, by means of chemical etching. The slits are separated by a 2 cm of free screen for standard OTR beam imaging. An aluminum layer is deposited onto the target by sputtering, and the reflectivity is enhanced by a factor of about 2. The main advantage of the silicon nitride with respect to SiO_2 [13] is a much less etching rate which preserves the silicon substrate from damages and makes the surface much more uniform.
A motorized actuator allows high precision positioning of the screen down to 1 μm and a very small movement for accurate centering of the slit with respect to the beam.

Fig. 4 – Diffraction Radiation target

The optical system layout is shown in Fig. 5. Radiation from the target is reflected by a mirror and sent through an optical system to the camera. Since the reflection power of the mirror surface is different for horizontal and vertical polarizations, and the component parallel to the incident plane (the horizontal one) is reduced, the effect is a non-perfect annular OTR angular distribution. Two lenses can be selected: an achromatic doublet to image the beam and a biconvex lens with broadband anti-reflection coating to produce the DR angular distribution. They have different focal lengths in order to focus on the same plane. Two interferential filters, at 800 nm and 550 nm and a Glan–Thomson polarizer may be inserted in the optical path. The positioning of these elements behind the lenses has been dictated by practical considerations due to the limited space. The effect of the polarizer is to lengthen the optical path, thus increasing the focal length in a range which is within the longitudinal movement of the camera.

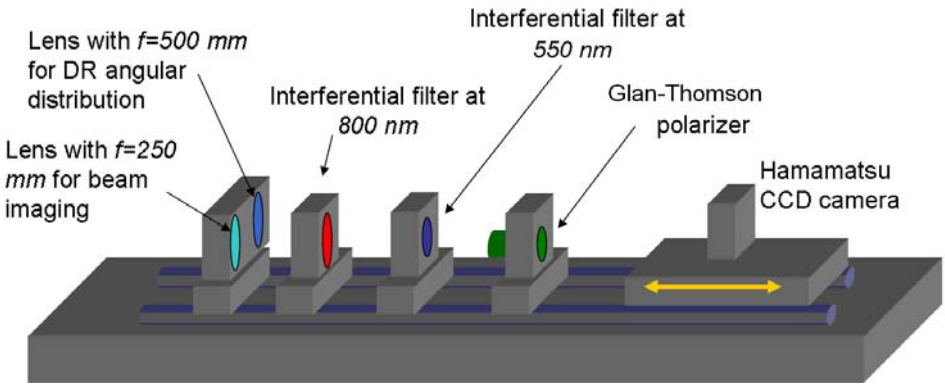

Fig. 5 – Sketch of the optical system

Due to the very low radiation intensity, a cooled, high sensitivity, 16-bit CCD camera (Hamamatsu C4742-98-LGLAG2) is used. The camera main features are a very high quantum efficiency in the whole visible spectrum, in particular at 800 nm, negligible thermal noise, and the long exposure times, up to 2 h. Let us note that since the camera is rotated by 90º, in the following pictures the vertical axis on the screen corresponds to horizontal one on the camera and vice versa. The optical system is remotely controlled by an electronic box, using CAN-bus modules, partially integrated in the linac control system and placed in the tunnel. The image acquisition and all related controls are driven via Firewire by a dedicated industrial PC located nearby and connected to the standard Ethernet network.

4 – First Results

The first measurement periods dedicated to the development of this instrument were performed with an electron beam energy of 620 MeV. With this relative low beam energy we did not expect accurate results of the ODR angular distribution measurements, but concentrated on the understanding of the synchrotron radiation background and developments on methods and tools to subtract it.
Indeed the synchrotron radiation background from the last dipole and the quadrupoles of the transfer line, some of them required a strong field, was higher than foreseen, because the light was collected by the highly reflective vacuum pipe and brought to the ODR screen with a large angular spread.

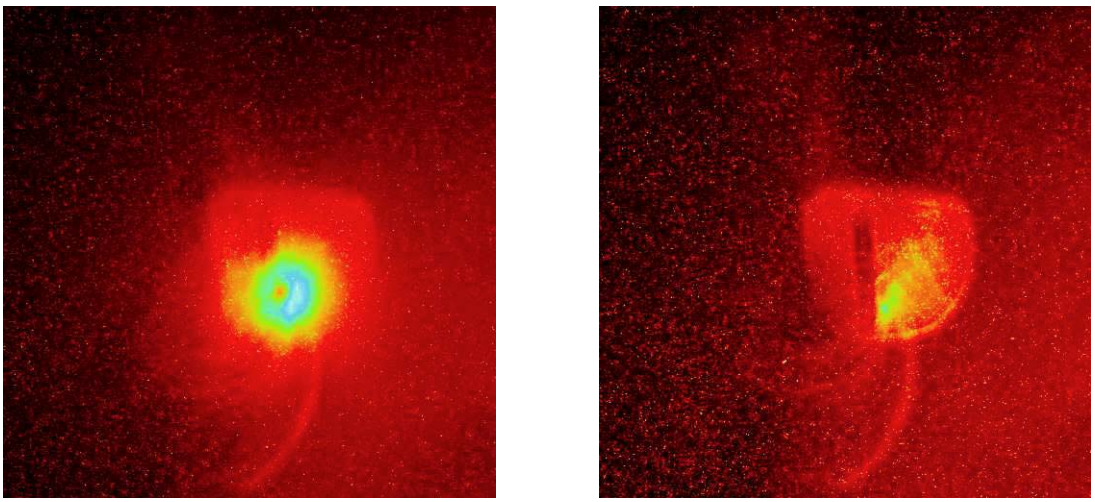

Fig. 6 – Pictures of OTR angular distribution (left) and SR background (right).

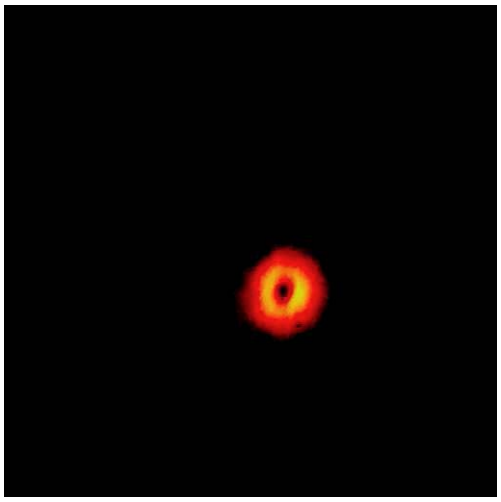

Fig. 7 – OTR angular distribution after background subtraction. 10 bunches, 0.3 nC per pulse, 2s exposure time.

The effect is shown in Fig. 6 where the OTR angular distribution is presented together with the background obtained while steering the beam away from the screen in order to avoid direct illumination.
After careful subtraction of synchrotron radiation background and hot spots due to x-rays, the resulting OTR angular distribution is shown in Fig. 7.
We applied the same background subtraction technique to the ODR measurement, where the signal-to-noise ratio is worse due to the lower ODR intensity. We started with a scan of the beam across the slit to verify the variation of the intensity in the interference fringes. A collection of background corrected ODR images taken during this scan is presented in Fig. 8.

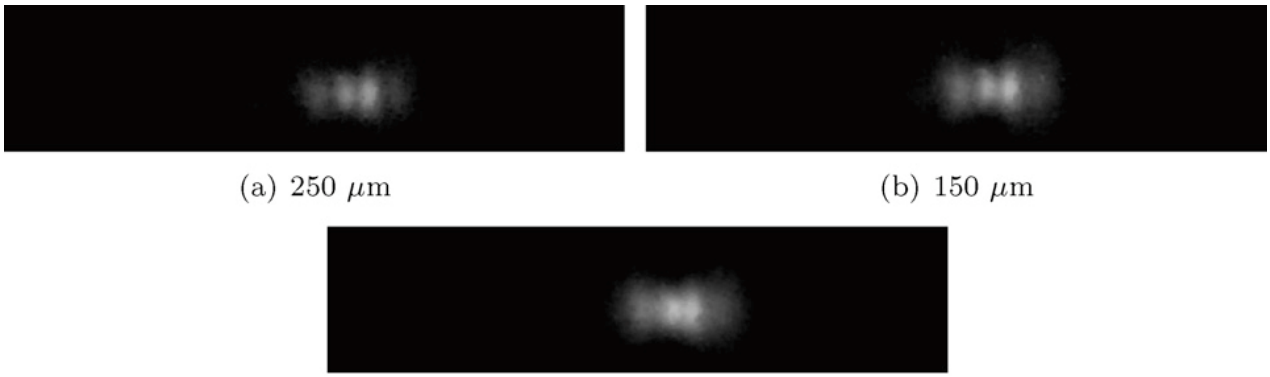

(a) 250 μm (b) 150 μm

(c) 50 μm

Fig. 8. Vertically polarized angular distribution for different positions of the beam within the slit: 250 μm corresponds to the beam centered in the slit aperture.

Some profiles of these distributions are shown in Fig. 9 together with theoretical predictions, demonstrating the capability of the experiment to resolve the decrease of the interference fringes visibility.

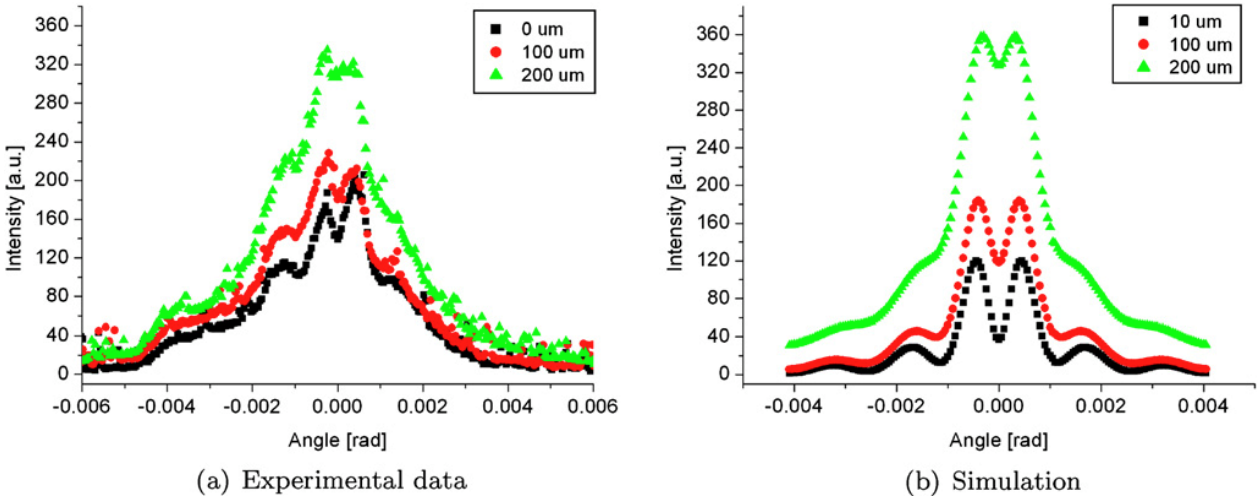

(a) Experimental data (b) Simulation

Fig. 9 - Angular distributions for different positions of the beam with respect to the slit center: 10 μm (black squares), 100 μm (red dots), 200 μm (green triangles). Both the polarizer and the 800 nm filter are inserted.

With an optimized beam in the slit center, we took a dedicated set of data together with the relevant background images, from which we derived the angular distribution shown in Fig. 10. The continuous curve is a simulation based on measured beam size and divergence, obtained via a quadrupole scan in the same beam time.

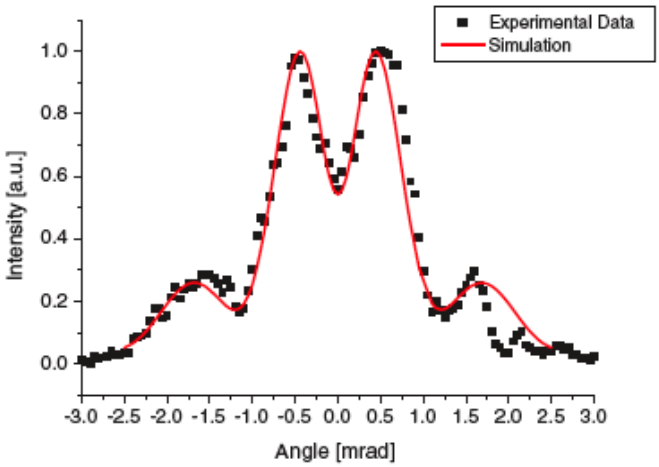

Fig. 10 - ODR angular distribution: 25 bunches per macropulse, 0.7 nC per bunch, 2 s exposure time, 5 Hz repetition rate, 0.5 mm slit. Polarizer and 800 nm filter are inserted.

With these results we have demonstrated that when a careful subtraction of the background is applied, the feature of ODR can be clearly evidenced [14], even at a beam energy lower than required.
However, the background is the most severe limitation of this technique.

5 – Optical Diffraction Radiation Interferometry (ODRI)

To reduce the effect of the synchrotron radiation background, we installed a stainless steel shield in front of the ODR screen with larger cuts in it: 2 mm for the 1 mm slit and 1 mm for the 0.5 mm one, c.f. Fig. 11.

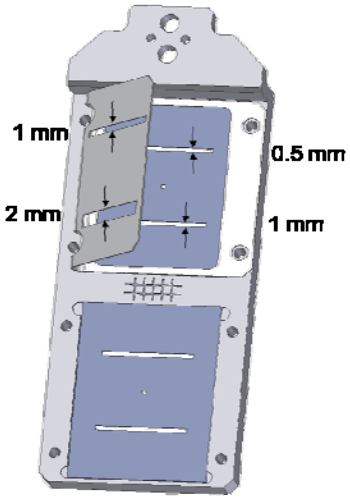

Fig. 11 – Sketch of the new screen together with shield.

To be effective in reducing the background, the cut in the shield cannot be too large. We chose a dimension for which ODR emitted in forward direction was strongly reduced, but still perceptible. In this way what we measured was the interference between the forward emitted ODR from the shield together with the backward emitted ODR from the screen. These two amplitudes have opposite signs and a phase difference given by

$$\phi = \frac{2\pi}{\beta}\frac{d}{\lambda}(1-\beta\cos\vartheta)$$

in which λ is the measured wavelength, β the normalized beam velocity, ϑ the radiation emission angle and d the distance between screen and shield. Due to the experimental geometry this distance depends on the horizontal beam position, but is between 10 and 20 mm.

In Fig. 12 we show the angular profiles of ODR produced independently by the shield and the screen together with the result of their interference simulated in the case of an energy of 920 MeV and a wavelength of 800 nm.

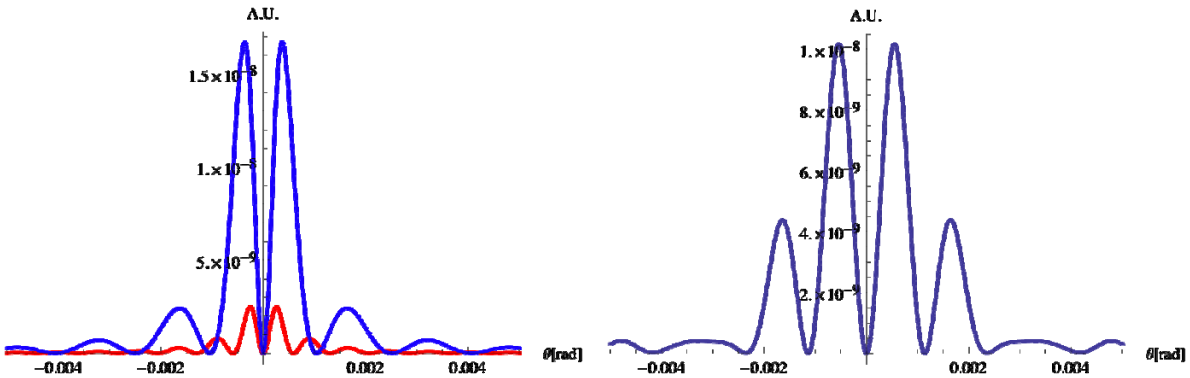

Fig. 12 – (*left*) ODR emitted independently by the shield (*red*) and the screen (*blue*); (*right*) ODR produced by the interference of the two amplitudes.

The ODR produced by the interference of the two amplitudes shows suppression of the central peaks and an enhancement of the side maxima.

6 – Recent Results

The second period of measurements have been carried out with a higher electron beam energy of about 900 MeV. First the electron beam transport was optimized to achieve as small as

possible transverse beam size on the location of our experiment. The beam image and the vertical profile are shown in Fig. 13 (top images). The rms vertical beam size, estimated by a Gaussian fit is 90 μm. After that we looked at the OTR angular distribution to obtain estimation of the beam energy and vertical angular divergence. The corresponding values are shown in Fig. 13 (bottom right image).

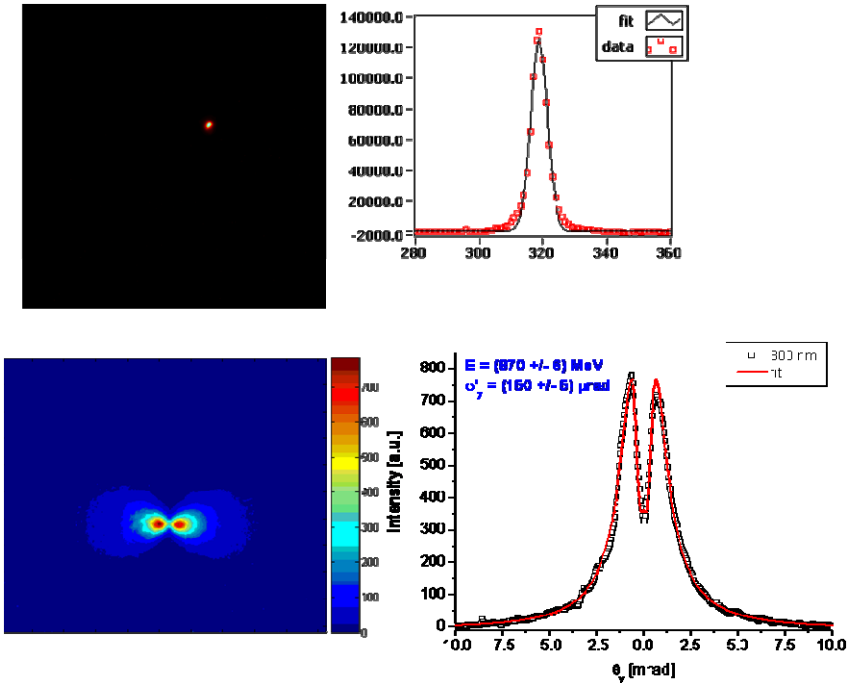

Fig. 13 – (*top*) OTR beam image and its projection;
(*bottom*) OTR angular distribution and its profile, fit to retrieve beam energy and beam angular divergence.

A complete transverse scan of the beam position in the slit aperture has been carried out by moving the slit respect to the beam position from one edge of the slit to the other one. The results are shown in figure 14 (left: ODRI angular distribution image, right: ODRI angular distribution profile). We moved in steps of 25 μm around the slit center. Due to the fact that both slits were not aligned with respect to each other, a different behavior of the experimental distributions was supposed while going from the center of the slit to one edge or towards the other.

A strong asymmetry is shown by the ODRI experimental distribution which can only be explained by assuming that the two half planes of the DR target are parallel but not perfectly coplanar. In this case, the field of a particle incident with angle α (in our case, $\alpha = \pi/4$) will be reflected by one half plane earlier than by the other. Under the approximations (1) $d \ll \gamma\lambda$ and (2) $\beta \approx 1$, the phase difference between the two fields amounts $4\pi d/\lambda cos(\alpha)$ with d the longitudinal difference between the two semi-planes.

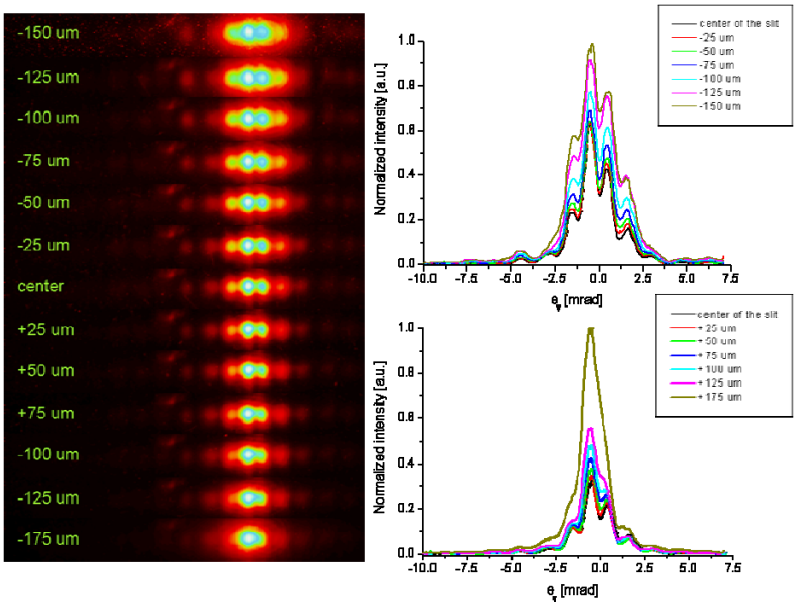

Fig. 14 – ODRI angular distribution image (*left*) and profile (*right*) for different impact parameters. For these ODRI measurements, FLASH was operated with 13 bunches per macropulse, 0.8 nC per bunch, 2 s exposure time, 5 Hz repetition rate, and 0.5 mm slit width. Polarizer and interference filter (800 nm) were inserted.

The experimental curve for the case of the beam going through the center of the 0.5 mm slit has been compared with theoretical calculations performed in a Monte-Carlo simulation assuming the transverse beam size, the angular divergence and the energy known, i.e. $\sigma_y = 90$ μm, $\sigma'_y = 150$ μrad, E = 870 MeV. The parameters varied were:

i) the phase difference between the two half planes of the 0.5 mm slit, which takes into account their non-coplanarity;
ii) the misalignment between the two slits;
iii) the phase difference between the two slits.

In the calculation we assumed a Gaussian distributed beam both in size and angular divergence.

In Fig. 15 the ODRI angular distribution is compared with the simulation assuming a misalignment between both slits of 130 μm, and a phase difference between the two half planes of the 0.5 mm slit corresponding to a misalignment of 70 nm.

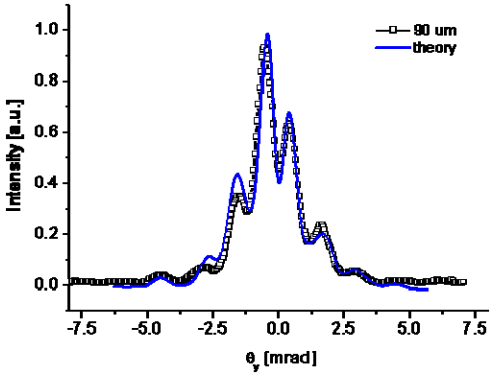

Fig. 15 – ODRI experimental angular distribution for a beam going through the 0.5 mm slit compared with the theoretical curve.

Fig. 16 shows measured OTR angular distributions at observation wavelengths of λ = 800 nm and 550 nm. As can be seen the angular distribution is independent on λ as expected from theory.

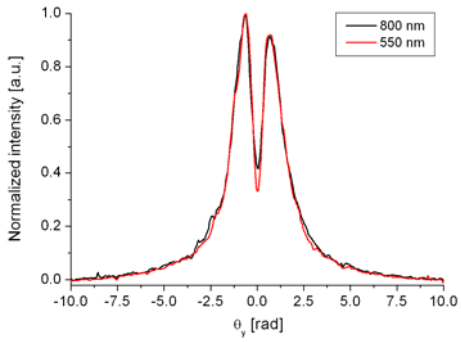

Fig. 16 – OTR experimental angular distribution for two different wavelengths.

The measurements have been repeated for a smaller transverse beam size (σ_y = 78 μm). In Fig. 17 an example of a comparison between the experimental ODRI angular distributions for the two different beam sizes is shown. The measurement demonstrates the sensitivity of the experiment even on smallest variations of the transverse beam size in the order of a few micrometer.

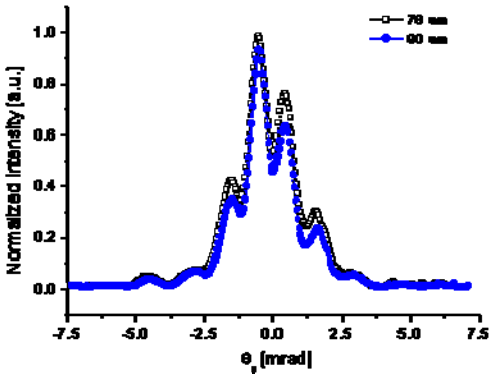

Fig. 17 – Comparison between ODRI angular distributions for two different transverse sizes.

The ultimate goal of our experiment is to determine the transverse projected emittance from the transverse beam size and angular divergence obtained by the OTR and ODRI analysis. The determination of the emittance from these two beam parameters is possible assuming that the beam size has its vertical waist located in the slit plane. With this assumption the emittance is estimated to be about 20 mm mrad. A quadrupole scan shown in Fig. 18 which was done as additional cross-check indicates consistency with the ODRI analysis and confirms the possibility to use this technique for precise beam characterization.

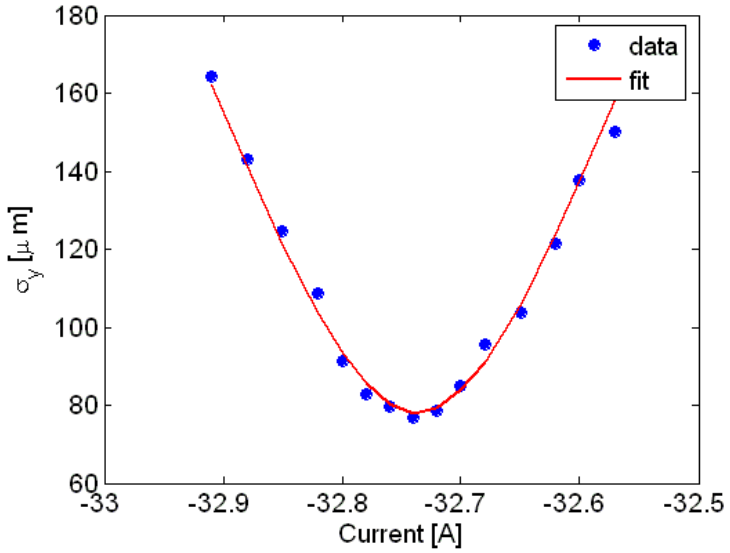

Fig. 18 – Quadrupole scan.

However, the vertical normalized emittance measured downstream the first accelerating module with the four-screen method results in a value of about 4 mm mrad. This discrepancy might be explained assuming an emittance degradation during the propagation through the "dogleg" of the dipole magnets that bring the beam into the by-pass line. We believe that this degradation is an effect of a mismatched line. This interpretation is also confirmed by the fact that the emittance we measure is strongly dependent on minimal changes on quadrupole settings.

8 - Conclusions

We have confirmed that ODR can be used as a non intercepting beam size diagnostics, allowing also the simultaneous measurement of the beam angular spread. We used a much more intense beam (up to 130 nC) than previously used at KEK [7], without any screen damage and with the total beam transported through the slit. The main drawback, i.e. the background of synchrotron radiation from bending and quadrupole magnets, was strongly reduced by means of a stainless-steel shield with a larger cut in front of the screen. Our new set-up using Optical Diffraction Radiation Interferometry (ODRI) provides an additional advantage: the interference fringes are much more visible and an easier centering of the beam is possible.
The evolution of our work has been documented by many seminars and presentations in international conferences [14], [15], [16], [17], [18], [19], [20].

References

[1] <www.linearcollider.org>.
[2] M.Altarelli et al. (Eds.), "XFEL: The European X-Ray Free-Electron Laser: Technical Design Report", DESY 2006-097.

[3] LCLS Conceptual design report <www-ssrl.slac.stanford.edu/lcls/cdr>.
[4] SPARC Group (LNF-INFN, Roma1-INFN, Roma2-INFN, ENEA, CNR, Milano-INFN), Technical design report, January 2004<www.lnf.infn.it/acceleratori/sparc/>.
[5] M. Castellano,
"A new non-intercepting beam size diagnostics using diffraction radiation from a slit",
Nucl. Instr. and Meth. Phys. Res. A394 (1997) 275.

[6] M. Castellano,
"Diffraction Radiation as a Non-Intercepting Diagnostics for TTF: the Bunch Length Measurement",
DESY Report TESLA 96-08.

[7] P. Karataev, S. Araki, R. Hamatsu, H. Hayano, T. Muto, G. Naumenko, A. Potylitsyn, N. Terunuma, J. Urakawa,
Phys. Rev. Lett. 93 (2004) 244802.

[8] A.H. Lumpkin, W.J. Berg, N.S. Sereno, D.W. Rule, C.-Y. Yao,
Phys. Rev. ST Accel. Beams 10 (2007) 022802.

[9] E. Chiadroni, PhD Thesis, DESY Report TESLA FEL 2006-9
(<http://flash.desy.de/reports_publications/tesla_fel_reports/tesla_fel_2006/index_eng.html>).

[10] M.L. Ter-Mikaelian,
"High-Energy Electromagnetic Processes in Condensed Media",
Wiley-Interscience, New York, 1972.

[11] M. Born, E. Wolf,
"Principles of optics",
Pergamon Press, 1965.

[12] W. Ackermann et al., Nature Photonics 1 (2007) 336.
[13] E. Cianci et al.,
"Micromachined silicon slit for beam diagnostic in particle accelerator",
Proc. SPIE, 4557, pp.242-249 (2001).

[14] E. Chiadroni et al.,
"Non-Intercepting Electron Beam Trasverse Diagnostics with Optical Diffraction Radiation at the DESY FLASH Facility",
Nucl. Instr. And Methods in Physics Research, B **266** (2008) p.3789-3796.

[15] E. Chiadroni, M. Castellano, A. Cianchi, K. Honkavaara, G. Kube,
"Status of the Electron Beam Transverse Diagnostics with Optical Diffraction Radiation at the DESY FLASH Facility",
International Conference on Charged and Neutral Particles Channeling Phenomena, S. Dabagov, Ed., Proceedings of SPIE Volume: 6634, 21 May 2007.

[16] E. Chiadroni, M. Castellano, A. Cianchi, K. Honkavaara, G. Kube,
"Non-Intercepting Electron Beam Transverse Diagnostics with Optical Diffraction Radiation at the DESY FLASH Facility",
Proceedings of the Particle Accelerator Conference 2007, Albuquerque, New Mexico, USA.

[17] A. Lumpkin, C.-Y. Yao, E.Chiadroni, M. Castellano, A. Cianchi,
"Considerations on ODR beam size monitoring for gamma = 1000 beams",
Proceedings of 2008 Beam Instrumentation Workshop, Lake Tahoe, California.

[18] E. Chiadroni, M. Castellano, A. Cianchi, K. Honkavaara, G. Kube,
"New Experimental Results with Optical Diffraction Radiation Diagnostics",
Proceedings of the 11th Particle Accelerator Conference (EPAC08), Genova, Italia.

[19] E. Chiadroni, M. Castellano, A. Cianchi, K. Honkavaara, G. Kube,
"New Experimental Results with Optical Diffraction Radiation Diagnostics",
International Conference on Charged and Neutral Particles Channelling Phenomena, Channeling08, Erice, Sicily.

[20] M. Castellano, E. Chiadroni, A. Cianchi,
"Diffraction Radiation as a diagnostics Tool at FLASH",
International Conference on Charged and Neutral Particles Channelling Phenomena, Channeling08, Erice, Sicily.